Lawrence Berkeley National Laboratory

Recent Work

Title

Detecting MALDI ions with a cryogenic detector

Permalink

https://escholarship.org/uc/item/4k97v1qb

Author

Benner, W. Henry

Publication Date

1997-09-12

eScholarship.org Powered by the California Digital Library
University of California

LBNL-40059

ERNEST ORLANDO LAWRENCE
BERKELEY NATIONAL LABORATORY

Detecting MALDI Ions with a Cryogenic Detector

W. Henry Benner, F. Zhong,
M. Frank, and S. Labov

Engineering Division

September 1997

Presented at the
14th International Mass Spectrometry Conference,
Tampere, Finland,
August 25–29, 1997,
and to be published in
the Proceedings

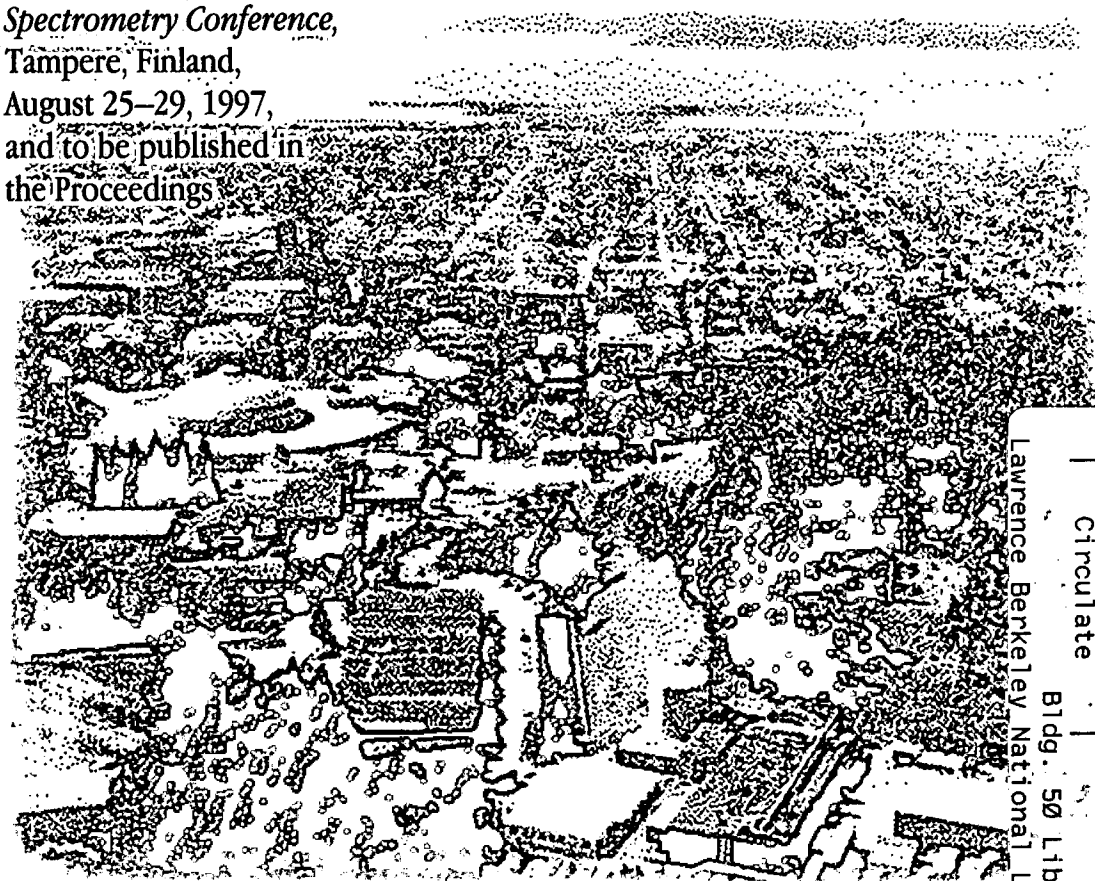

REFERENCE COPY
Does Not
Circulate
Copy 1
Bldg. 50 Library - Ref.
Lawrence Berkeley National Laboratory
LBNL-40059

DISCLAIMER

This document was prepared as an account of work sponsored by the United States Government. While this document is believed to contain correct information, neither the United States Government nor any agency thereof, nor The Regents of the University of California, nor any of their employees, makes any warranty, express or implied, or assumes any legal responsibility for the accuracy, completeness, or usefulness of any information, apparatus, product, or process disclosed, or represents that its use would not infringe privately owned rights. Reference herein to any specific commercial product, process, or service by its trade name, trademark, manufacturer, or otherwise, does not necessarily constitute or imply its endorsement, recommendation, or favoring by the United States Government or any agency thereof, or The Regents of the University of California. The views and opinions of authors expressed herein do not necessarily state or reflect those of the United States Government or any agency thereof, or The Regents of the University of California.

Ernest Orlando Lawrence Berkeley National Laboratory
is an equal opportunity employer.

DISCLAIMER

This document was prepared as an account of work sponsored by the United States Government. While this document is believed to contain correct information, neither the United States Government nor any agency thereof, nor the Regents of the University of California, nor any of their employees, makes any warranty, express or implied, or assumes any legal responsibility for the accuracy, completeness, or usefulness of any information, apparatus, product, or process disclosed, or represents that its use would not infringe privately owned rights. Reference herein to any specific commercial product, process, or service by its trade name, trademark, manufacturer, or otherwise, does not necessarily constitute or imply its endorsement, recommendation, or favoring by the United States Government or any agency thereof, or the Regents of the University of California. The views and opinions of authors expressed herein do not necessarily state or reflect those of the United States Government or any agency thereof or the Regents of the University of California.

LBNL-40059

Detecting MALDI Ions with a Cryogenic Detector

W. Henry Benner and F. Zhong

Engineering Division
Ernest Orlando Lawrence Berkeley National Laboratory
University of California
Berkeley, CA 94720

M. Frank and S. Labov

Lawrence Livermore National Laboratory
700 East Avenue
Livermore, CA 94550

September 1997

This work was supported by the Director, Office of Energy Research, Office Health and Environmental Research, Human Genome Program, of the U.S. Department of Energy under Contract No. DE-AC03-76SF00098.

Recycled Paper

Detecting MALDI Ions with a Cryogenic Detector

W. Henry Benner and F. Zhong
Lawrence Berkeley National Laboratory
1 Cyclotron Rd., Berkeley, CA 94720
and
M. Frank and S. Labov
Lawrence Livermore National Laboratory
700 east Ave., Livermore, CA 94550

Progress in cryogenic detector technology has led to the development of new devices appropriate for use as ion detectors. We have recently begun to evaluate one type of cryogenic detector called a superconducting tunnel junction (STJ) detector. Initial tests were conducted by replacing a microchannel plate ion detector in a matrix-assisted-laser-desorption time-of-flight mass spectrometer (MALDI-TOF-MS) with a STJ detector. In those initial tests we showed that 1) the STJ detector produces pulses appropriate for timing large ions and 2) the height of the pulses is proportional to ion energy and thus useful for deducing ion charge. STJ detectors are energy detectors and when operated in pulse detection mode, produce signals of individual ions, presumably with a detection efficiency close to 100 percent. Whereas MCP's detect ions via secondary ionization processes, the energy response of a STJ detector provides a way to detect massive ions that do not produce secondary ions efficiently upon impact with MCP's. For this reason, the current attraction to STJ detectors is primarily for massive ions. We now report additional STJ ion energy measurements that help to reveal some aspects of ion fragmentation in MALDI mass spectrometry.

The height of the output pulse from a STJ detector is related approximately linearly to ion energy, thus doubly charged ions in a MALDI-TOF-MS produce pulses about twice as large as singly charged ions. Cryogenic detectors show excellent energy resolution for X rays but poorer energy resolution is observed when MALDI ions are analyzed. The cause for the poor energy resolution of MALDI ions is not fully understood, nevertheless it appears feasible to use STJ detectors to study the energy distribution of MALDI ions. The detectors appear to be sensitive enough to measure individual ion impacts and processes which influence ion energy such as in-source fragmentation and the deficit of ion energy caused by accelerating ions through a MALDI plume. In this study, we show how a STJ detector can be used to measure the time of flight of macroglobulin ions (725, 000 Daltons), determine ion charge using detector pulse height and investigate in-source fragmentation patterns.

The STJ detector used in this study has been described in detail.[1,2] It consists of two thin overlapping Nb films separated by a 20 Å film of Al_2O_3. The device is operated at 1.3 K with a small bias voltage applied to the Nb films. In the superconducting state (< 9 K for Nb), conduction electrons in the Nb films associate as Cooper pairs. The oxide layer electrically isolates the Nb films and acts as a tunneling barrier for Cooper pairs. When energy is deposited into the Nb films by an impacting ion, the Cooper pairs dissociate into quasiparticles (electrons)

which tunnel through the Al_2O_3 layer. The result is a tunneling current pulse. The magnitude of the current pulse is proportional to the number of broken Cooper pairs, which in turn is proportional to the amount of energy deposited into the Nb film. Fig. 1 shows a sequence of current pulses resulting when MALDI ions generated by a single laser shot hit the detector. Even though the active area of the STJ detector is only 200 by 200 μm, many ions hit the detector following each laser shot. This particular TOF spectrum is presented show the variation in STJ detector pulse height attributable to ion energy. Several of the pulses in this spectrum are labeled to identify the ions that produced the pulse. The identity of these ions was determined by flight time. It can be seen that the pulse produced by the doubly charged human serum albumin (HSA) ion is about twice as tall the singly charged HSA and the singly charged HSA dimer ion. The identity of the ions that caused the other pulses is presumably singly charged matrix ions.

The customary way to collect MALDI TOF spectra is to digitize the output from a MCP detector for several hundred μs following the laser shot and then add and average spectra from many laser shots. Peaks in these averaged TOF spectra are used to identify analyte ions in a sample. This same procedure can be used to acquire averaged spectra with a STJ detector. An example of such a spectrum is shown in Fig 2 for a sample of macroglobulin in sinapinic acid matrix. Peak assignments based on ion flight times show that the macroglobulin molecular ion was detected with the STJ detector. Macroglobulin is comprised of tetrameric subunits that break apart during MALDI sample preparation unless they are cross-linked together. The sample used in Fig. 2 was chemically cross-linked with acetaldehyde because the intact macroglobulin molecular peak was not observed unless the macroglobulin was cross-linked.. The efficiency of the cross-linking procedure is not known, therefore the relative peak heights or ions in this spectrum should not be used to evaluate the efficiency for creating and detecting intact macroglobulin ions. Cross-linking shifts the position of the macroglobulin peak to higher mass (725 kDa vs. 750 kDa). This mass shift is inconsequential to the purpose of this analysis because we wished only to demonstrate the detection of large ions with a STJ detector and not the determination of the exact mass of macroglobulin. Peaks in this mass spectrum could be assigned by their flight times to $½ M^{2+}$ and $½ M^{+}$ where M represents the macroglobulin tetramer.

An informative way to display STJ detector signals is to plot time-of-flight vs. detector pulse height for individual ions. The upper panel in Fig. 3 shows this type of scatter plot for MALDI ions of macroglobulin in sinapinic acid. Clusters of data points in this figure correspond to a variety of different types of macroglobulin ions. Some of the clusters correspond to singly- or multiply-charged unfragmented macroglobulin ions while other clusters are assigned to multiples of the tetrameric units carrying a range of charge. Still other clusters are due to matrix ions and randomly sized fragments of macroglobulin which are not tetrameric subunits.

The lower panel in Fig. 3 is a histogram of detector pulses selected by making a pulse height cut. Pulses less than 250 mV in amplitude, corresponding to singly charged ion pulses, were selected from the data presented in the upper panel of Fig 3 and accumulated into discrete TOF bins. The pulse height selection process improves the visibility of the TOF of singly charged ions. In addition to the peaks assigned to M^{+} and $½ M^{+}$, singly charged matrix ions and singly charged clusters of matrix ions appear at flight times less than about 200 μs. The gap between the peaks at 50 μs and 150 μs is an artifact caused by changing the voltage applied to the deflection plates in

the flight tube. Additional pulse height cuts can be made to select ions carrying multiple charges but they are not presented here because of page limitations.

Careful examination of the clusters in Fig. 3 indicates that the lower region in many of the clusters are shifted towards shorter flight times. In the extreme, as observed for the cluster at around 450 μs, this shift causes the cluster to have a crescent shape. One explanation for the crescent shape involves in-source fragmentation. To examine the possible cause for the shape of this cluster, we begin by assuming that a singly charged analyte ion breaks into two fragments, one charged and one neutral, before it passes through the grounded grid in the MALDI acceleration region. Depending on where fragmentation occurs in the source, the fragment ion could acquire a significantly higher velocity than the analyte ion and lead to peak broadening.

Although the flight times of all fragment ions can be calculated, here we consider only singly charged ions, and use the following equations:

consider : $M^+ \rightarrow m_1^+ + m_2^\circ$

$$TOF_{m_1^+} = TOF_M \left(u + \frac{(1-u)M}{m_1^+}\right)^{-1/2}$$

$$u = \frac{x}{d} \bullet U$$

where $TOF_{m_1^+}$ = flight time of charged fragment with mass m

TOF_M = flight time of analyte molecular ion with mass M

U = acceleration voltage

d = distance between source plate and grounded grid

x = distance from source plate to where fragmentation occurs

Flight time distributions for fragment ions with mass 0.01M, 0.02M, 0.03M ... 0.99M were calculated for various values of x. Resulting TOF distributions were then compared to the experimental data and a good match was found for x = 0.93d, as shown in Fig. 4. When the plot in Fig. 4 is compared to the cluster of points located around a flight time of about 625 μs in Fig. 3, corresponding to the singly charged fragments of the 750 kDa macroglobulin molecular ion, it can be concluded that the model accounts for the crescent shape of the cluster. The model can also be used to describe some of the other clusters seen in the upper panel in Fig. 3.[3] The crescent shape is a result of the fact that the fragment ions have shorter flight times than analyte ions and also because they also carry less energy than singly charged ions accelerated through U. For the cluster at 625 μs, the model indicates that fragmentation occurs at a position corresponding to a large value of u (such as 0.93U). This means that fragmentation occurs as the ions approach the grid. Presently, we do not understand why fragmentation occurs at this location. We plan to study this phenomenon in future experiments and investigate the influence of the grid. The distortion of the electrical field gradients near the grid could play a role in the fragmentation process.

In conclusion, the energy response of the STJ detector not only provides a way to assign charge to ions but also provides a way to examine fragmentation patterns for MALDI ions. The simple model described above appears to account for the flight times and expected energy of the ions that lead to clusters of crescent shaped data points. Work is under way to investigate the fragmentation of multiply charged ions.

Figure captions

Fig. 1. Tunneling current pulses produced by MALDI ions from a single laser shot. The sample is human serum albumin (HSA) in sinapinic acid. Acceleration voltage is 30 kV.

Fig. 2. Mass spectrum of cross-linked macroglobulin ("Mac", 750 kDa) in sinapinic acid. TOF spectra from 962 laser shots were averaged. Acceleration voltage is 30 kV.

Fig. 3. The upper panel shows a scatter plot of flight time vs. STJ detector output pulse height. When a pulse height cut is made to exclude detector pulses greater than 250 mV (corresponding to the horizontal line at 65 channels in the upper panel), pulses for singly charged ions are selected. The horizontal lines help to distinguish multiply charged ions. A histogram for the flight times of singly charged ions is shown in the lower panel. Acceleration voltage is 30 kV.

Fig. 4. A plot of model calculations used to predict the flight times of fragment ions with 30 keV. The point labeled M^+ corresponds to the flight time of the intact molecular ion. The line of points extending from this point towards shorter flight times describes the flight time of fragment ions forming at x/d = 0.93. Depending on fragment ion mass, indicated with labels such as 0.05M along this curve, flight time distributions produce clusters of points similar to the crescent shaped cluster in the upper panel of Fig. 3. The neutral fragments (m_o), regardless of their mass, have flight times related to the velocity of the molecular ion at the time of fragmentation and appear as a vertical line in this plot because x/d is constant and equals 0.93U.

---

[1] M. Frank, C.A. Mears, S. Labov, W.H. Benner, D. Horn, J.M. Jaklevic and A.T. Barfknecht, High-Efficiency Detection of 66,000 Da Protein Molecules using a Cryogenic Detector in a Matrix-Assisted-Laser-Desorption-Ionization Time-of-Flight Mass Spectrometer, Rapid Commun. Mass Spec., 1996, 10, 1946-1940.

[2] W.H. Benner, D. Horn, J.M. Jaklevic, M. Frank, C.A. Mears, S. Labov, A.T. Barfknecht, Simultaneous Measurement of Flight Time and Energy of Large Matrix-Assisted-Laser-Desorption Ionization Ions with a Superconducting Tunnel Junction Detector, J. Am. Soc. Mass Spectrom., 1997, 8, 1094-1103.

[3] M. Frank, S. Labov and W.H. Benner, in preparation for Rapid Commun. Mass Spec.

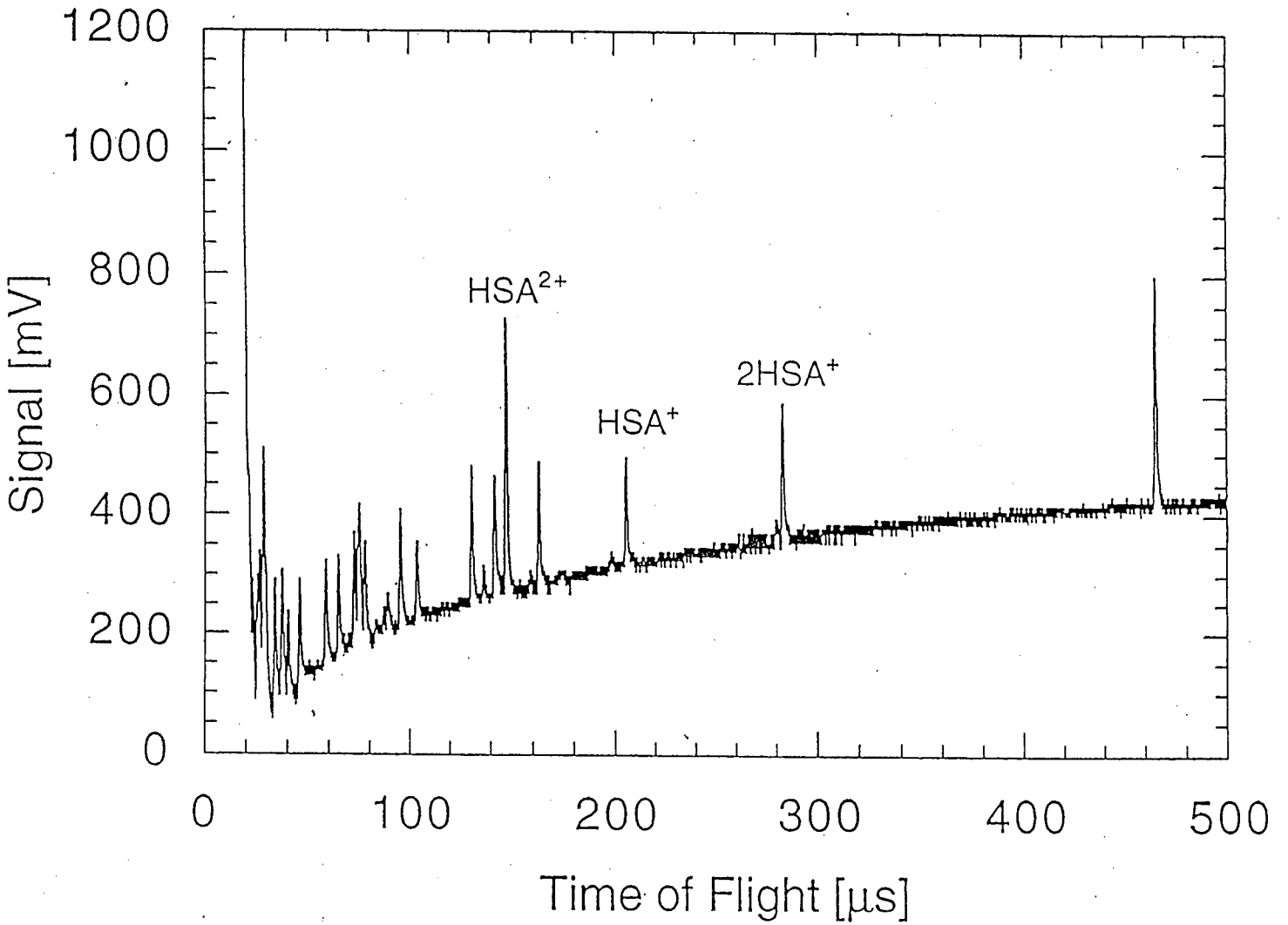
1200
1000
800
600
400
200
0
Signal [mV]
HSA2+
HSA+
2HSA+
0
100
200
300
400
500
Time of Flight [µs]

Figure 1

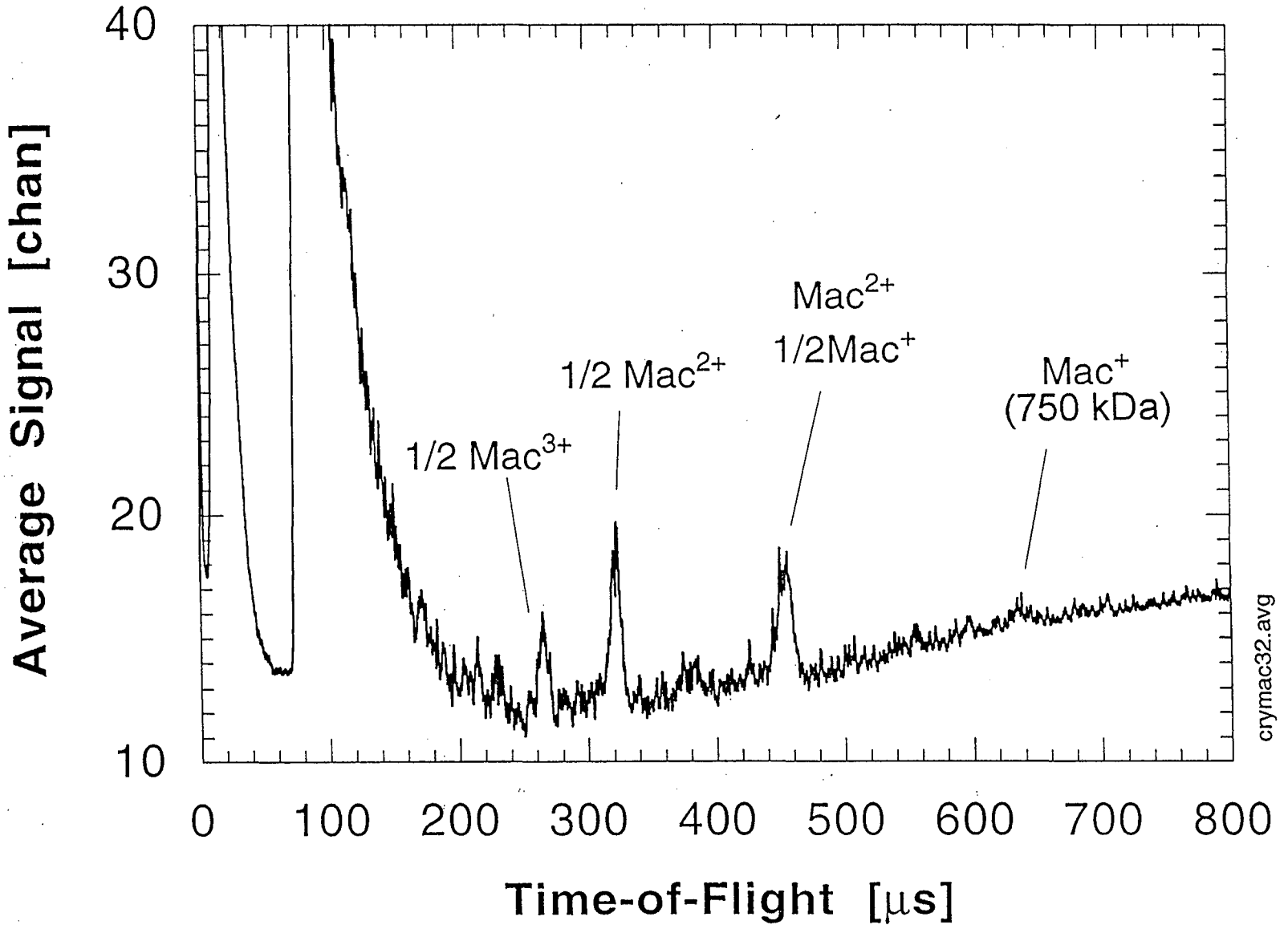
Average Signal [chan]
40
30
20
10
0
100
200
300
400
500
600
700
800
Time-of-Flight [μs]
1/2 Mac3+
1/2 Mac2+
Mac2+
1/2Mac+
Mac+
(750 kDa)
crymac32.avg

Figure 2

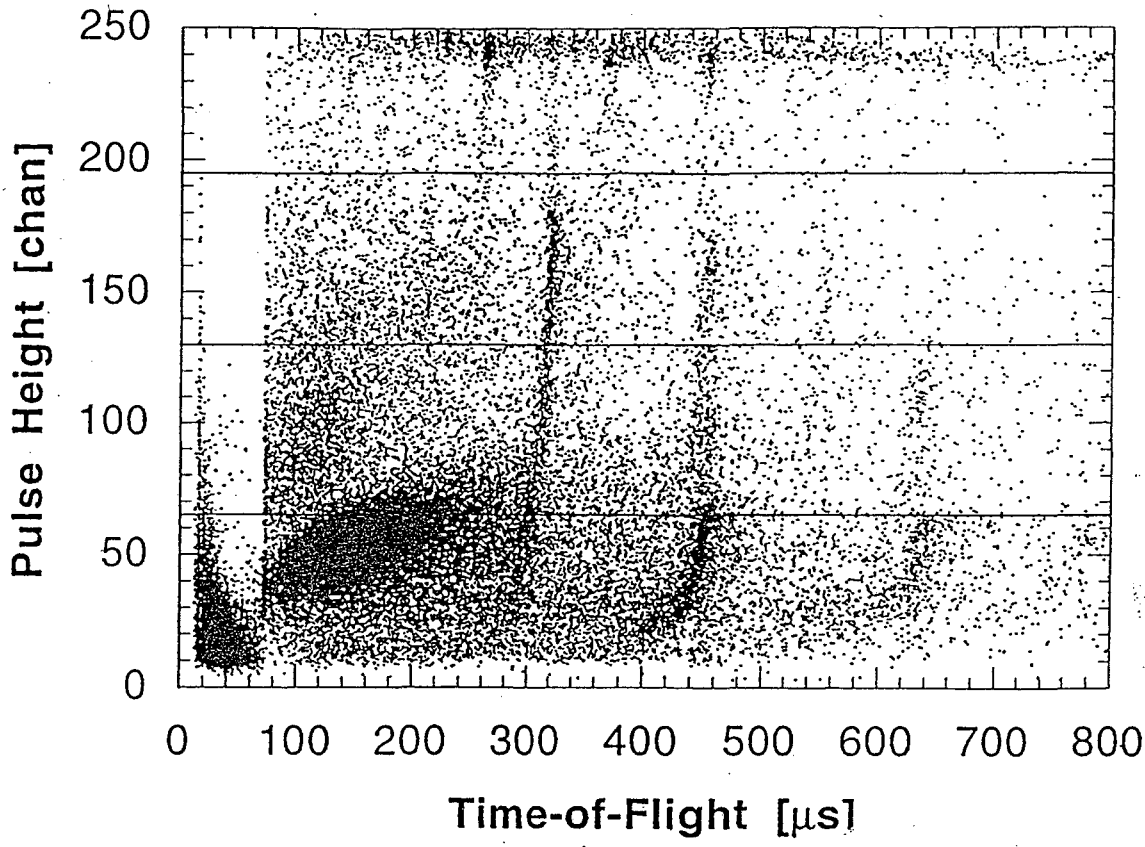
Pulse Height [chan]
250
200
150
100
50
0
0
100
200
300
400
500
600
700
800
Time-of-Flight [μs]

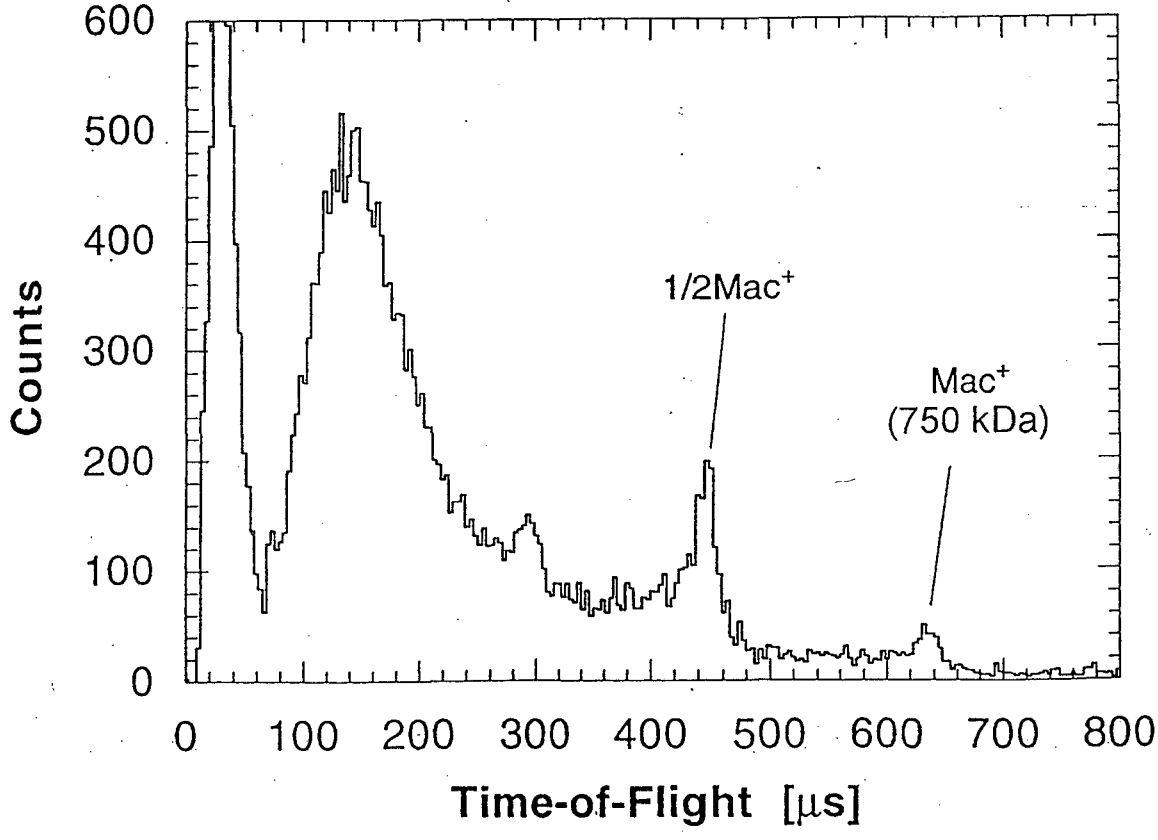
Counts
600
500
400
300
200
100
0
1/2Mac+
Mac+
(750 kDa)
0
100
200
300
400
500
600
700
800
Time-of-Flight [μs]

Figure 3

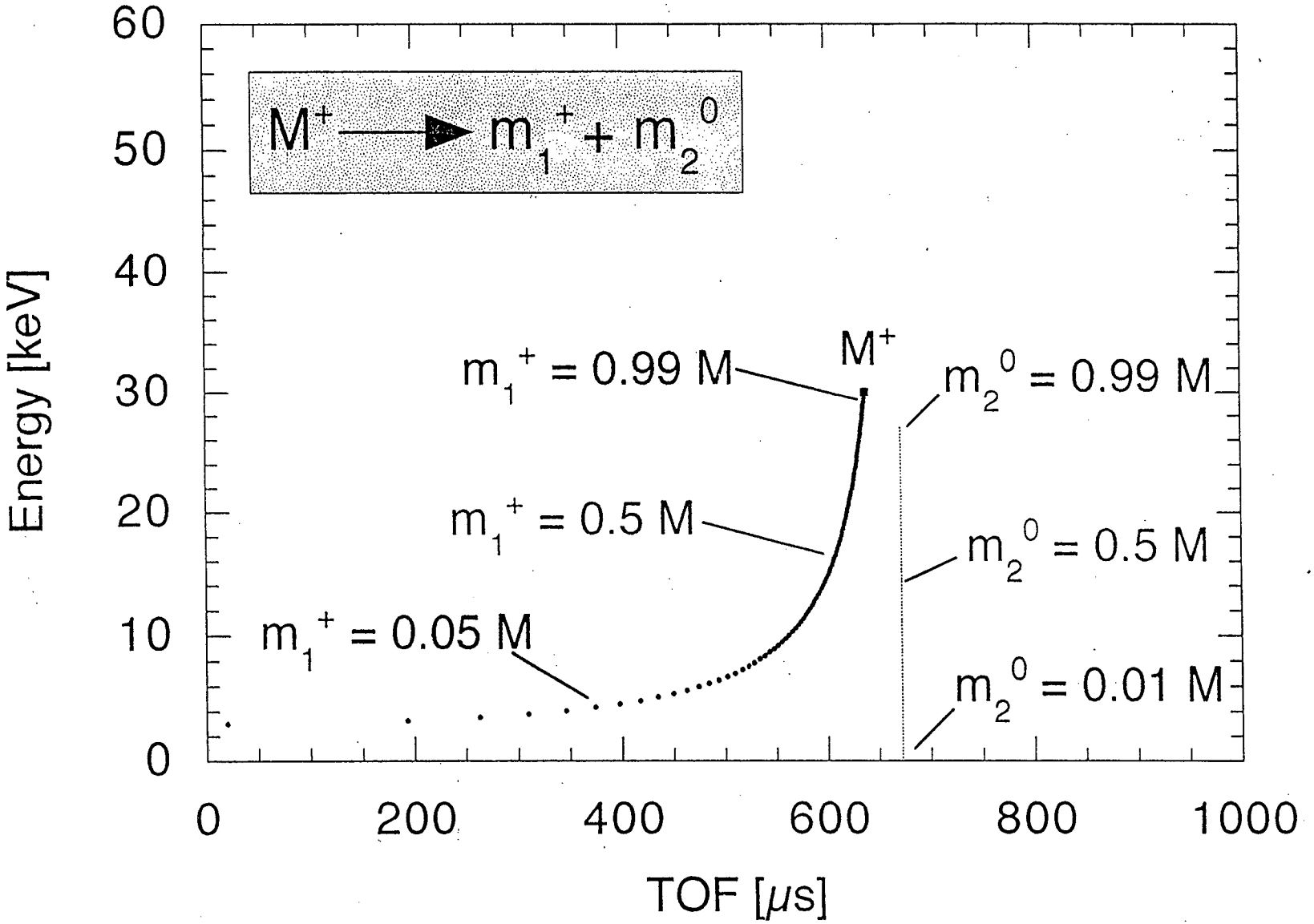
M+ → m1+ + m2 0
m1+ = 0.99 M
m1+ = 0.5 M
m1+ = 0.05 M
M+
m2 0 = 0.99 M
m2 0 = 0.5 M
m2 0 = 0.01 M
Energy [keV]
TOF [μs]
0
10
20
30
40
50
60
0
200
400
600
800
1000

Figure 4

Ernest Orlando Lawrence Berkeley National Laboratory
One Cyclotron Road | Berkeley, California 94720

Prepared for the U.S. Department of Energy under Contract No. DE-AC03-76SF00098